

ADSORPTION OF HORSE METHEMOGLOBIN ON BIOACTIVE GLASS AT HIGH SALT CONCENTRATION, STUDIED BY EPR AND FTIR SPECTROSCOPY

CRISTINA GRUIAN^{a, b}, HEINZ-JÜRGEN STEINHOFF^a,
SIMION SIMON^b

ABSTRACT. Although protein adsorption has been intensively studied in the last years, conformational changes which are likely to appear on the structure of the protein upon adsorption are difficult to evidence directly. Combined SDSL and EPR spectroscopy were applied to study adsorption of horse methemoglobin on bioactive glass in solution with high salt concentration (500mM NaCl). Further studies using FTIR spectroscopy aimed at identifying changes in the secondary structure of the protein upon the adsorption process. EPR spectra of methemoglobin spin labeled at position β -93 in solution were compared to those obtained after adsorption to extract structural information. A consistent analysis of EPR spectra revealed that the adsorption of methemoglobin is influenced by the chemical treatment applied to the surface of bioactive glass. From the FTIR spectra details concerning the changes of secondary structure of the protein after 2 hours of sample immersion in protein solution were obtained.

Keywords: *site-directed spin labeling, FTIR spectroscopy, protein adsorption, bioactive glasses*

INTRODUCTION

Protein adsorption and subsequent changes in their conformation are known to be the first biomechanical events taking place at the surface of an implant after implantation and determinants for further physicochemical interactions [1]. Thus, the first step in evaluating the blood and tissue compatibility of any medical device is to study its behavior in terms of interactions with proteins. The total amount of adsorbed protein as well as the overall protein-implant surface area interactions are of primary importance for the biocompatibility of a bioengineered material. It was also shown that the ionic strength of the solution influences the adsorption rate and the stability of protein

^a Department of Physics, University of Osnabrueck, 49069 Osnabrueck, Germany

^b Faculty of Physics, Babes-Bolyai University, 400084, Cluj-Napoca, Romania,
simion.simon@phys.ubbcluj.ro

binding [2-4]. Previous experiments conducted in our group have shown that low salt concentration positively influences the stability of methemoglobin adsorption on the type of bioactive glass (BG) used in this study (C. Gruian, H.J. Steinhoff, S.Simion - unpublished).

Other studies have shown that the use of protein coupling agents allows the control of protein release kinetics and maintains almost completely the native protein structure [5,6]. However, it is necessary to apply a certain chemical treatment to the surface for maintaining the protein-binding ability of the BG [7]. In this study the bioactive glass was silanized with 3-aminopropyl-triethoxysilane (APTS) [8] and subsequently modified with the protein coupling agent glutaraldehyde (GA).

Various techniques have been used to analyze secondary protein structures but they are not easily applicable to proteins that are adsorbed on solid surfaces so it is difficult to obtain structural information for adsorbed proteins. Many studies have used FTIR spectroscopy as a surface-sensitive technique to investigate protein structure because it has a high sensitivity to examine the structure of proteins in solution [9-11] and on surfaces [12-15]. Therefore, we investigated the conformational changes of horse methemoglobin during the adsorption on BG by using Fourier transform infrared (FTIR) spectroscopy and electron paramagnetic resonance (EPR) in combination with spin labeling. Changes in the secondary structure of the protein during the adsorption on the BG treated with GA were monitored by means of FTIR spectroscopy. In the amide I region, each type of secondary structure gives rise to a different C=O stretching frequency due to unique molecular geometry and hydrogen bonding pattern. Therefore, the observed amide bands are composed of several overlapping components representing helices, β -sheets, turns and random structures [16,17]. Moreover, from the amide I intensity we could monitor protein adsorption in time, until the surface was saturated.

Until now EPR was rarely used for studying the interaction between proteins and solid surfaces. Yet, the studies carried out to investigate the protein adsorption onto planar lipid bilayers [18, 19] or the partial unfolding of lysozyme on quartz [20] showed that this technique can successfully monitor the structural changes of a protein adsorbed to a solid surface. In this purpose, we introduced a spin label at position β -93 in methemoglobin [21]. It is important to mention that methemoglobin consists of four subunits: two α types and two β types. In each position β -93 the protein has a cysteine which was labeled with (4-(2-Iodoacetamido)-2,2,6,6-tetramethyl-1-piperidinyloxy) (JAA) (figure1).

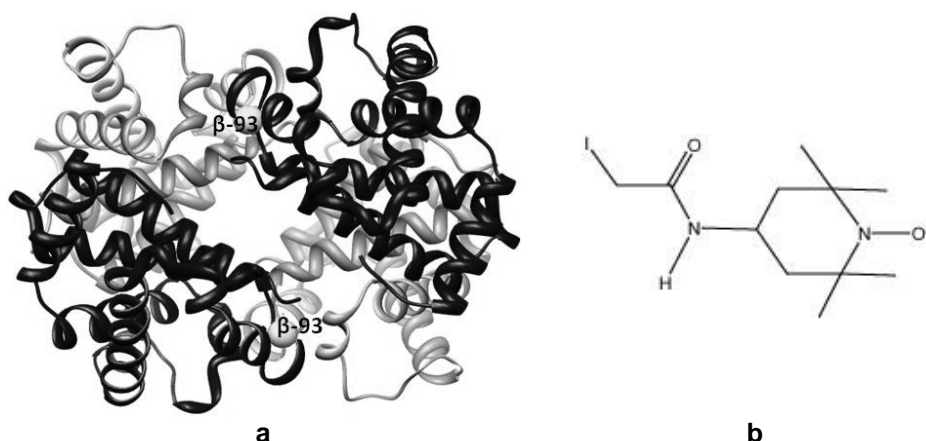


Figure 1 **a)** Structure of methemoglobin obtained by X-ray crystallography (2ZLU from Protein Data Bank). The α - and the β -chains are colored in different shades of grey. The native cysteins from position β -93 which were mutated to Cys and spin labeled with JAA are indicated as spheres. **b)** Structure of 4-(2-Iodoacetamido)-2,2,6,6-tetramethyl-1-piperidinyloxy spin label.

From the corresponding continuous wave (cw) EPR spectrum information about the nitroxide side chain mobility was obtained [21,22]. The mobility analysis is based on the fact that the room temperature EPR spectral line shape is sensitive to the reorientational motion of the nitroxide side chain due to partial motional averaging of the anisotropic components of the g- and hyperfine tensors. Further on, the distance between spin labels in the frozen state was determined by using pulse EPR DEER (double electron electron resonance) [23], to test whether the structure in close vicinity to amino acid position β -93 unfolds or if the protein keeps its native conformation upon adsorption.

RESULTS AND DISCUSSION

Cw-EPR spectra of methemoglobin recorded before and after adsorption on BG substrate are shown in figure 2a. It is important to mention that for all EPR spectra the measurements were performed in buffer solution, in order to monitor the protein behavior in its native environment.

X-band cw-EPR spectrum of methemoglobin in solution consists in two components with different mobility: an immobile component (arrow 2 in figure 2) which was best interpreted by Moffat [31] as corresponding to spin labels trapped in a protein pocket, and a mobile component (arrow 1 in figure 2) which correspond to the surface exposed spin labels. After adsorption, the equilibrium between the two components is significantly shifted towards the immobile one, indicating an increase in spin label immobilization due to

protein adsorption on the BG substrate [32]. The fractions of immobilized spin labels depicted in figure 2 were determined from simulations of cw-EPR spectra, using the Freed method [33]. This immobilization was even more pronounced on the BG treated with GA, a situation which can be explained if we assume that GA induces polymerization of methemoglobin when the protein is attached on the BG.

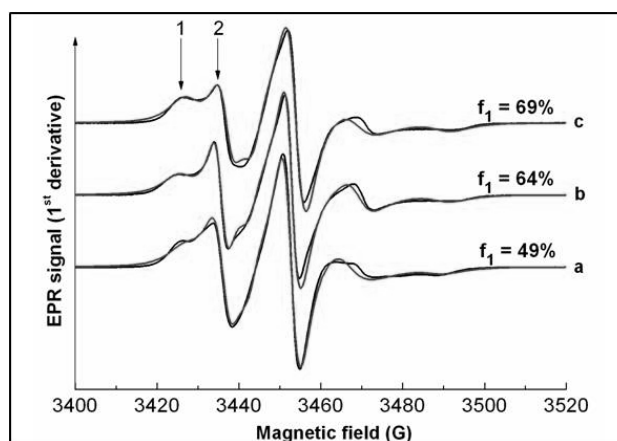


Figure 2. X-band cw-EPR spectra of horse methemoglobin spin-labeled in position β -93* recorded at room temperature; the black lines correspond to the spectra recorded in solution before (a) and after adsorption on the BG without GA (b) and with GA (c). The grey lines represent the best fit of the simulated spectra. The immobile and mobile components are indicated by arrows 1 and 2 respectively.

The information obtained from cw-EPR spectra is not sufficient to characterize protein adsorption in terms of structural changes; therefore, we performed pulse DEER EPR measurements. Figure 3 illustrates the experimental DEER time traces and the results after analysis with Tikhonov regularization (L-curve method) in DeerAnalyses2009 [30]. A first observation is that both DEER spectra recorded in adsorbed state have a very low modulation depth (<0.1 in case of BG without GA and 0 for BG treated with GA).

It is clear that when the protein is attached on BG a smaller number of spins have dipolar-dipolar interaction, compared with the protein in solution. We can explain this by assuming that a small part of methemoglobin dissociates upon adsorption. However, experiments conducted in our group have shown that this behavior is more pronounced when the solution has 50 times lower salt concentration (C. Gruian, H.J. Steinhoff, S.Simion, unpublished). Although electrostatic interactions have been proposed to dominate the protein-surface interaction [34], for the experimental conditions used here this balance is not in favor of the electrostatic interaction because of the high

salt concentration of the solution. Because protein dissociation was found to be less pronounced than in low salt conditions, one can conclude that electrostatic interactions play an important role in the dissociation of methemoglobin observed when the protein is adsorbed on the bioactive glass.

On the other hand, the total absence of modulation in the DEER signal on the BG treated with GA can be attributed also to a homogenous spatial distribution of the spin labels in the sample, as a consequence of polymerization induced by GA. We assume that in this case, both effects (dissociation and polymerization of the protein) are contributing to the overall DEER signal. Hence, after analysis with Tikhonov regularization a distance distribution could be obtained only for the protein in buffer solution and for protein adsorbed on BG without GA (figure 3). The C β -C β distances between the β -93 sites derived from the structures of the hemoglobin in solution and in the adsorbed state revealed a defined distance distribution, with a major distance at 24.8 Å in solution and 35 Å in adsorbed state. This increasing of major maximum in distance distribution suggests that the two β chains are slightly apart for the protein in adsorbed state. Projected on the protein, this means that in adsorbed state the tetrameric structure adopts a conformation which is slightly unfolded, as a consequence of interaction between protein and BG surface.

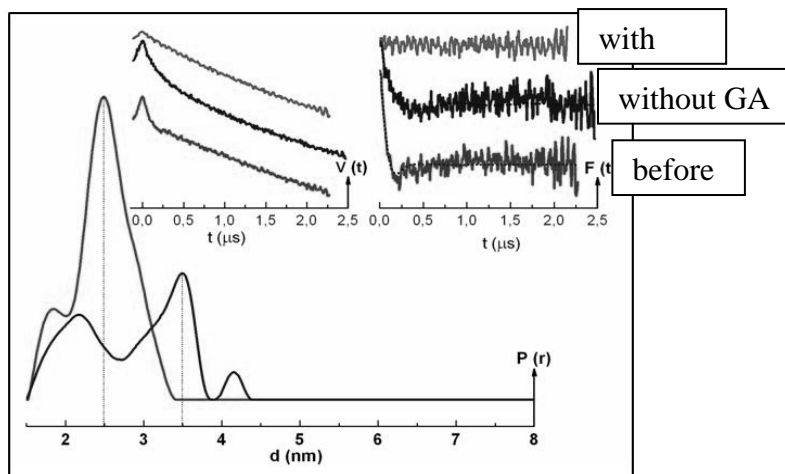


Figure 3 DEER analysis of methemoglobin in solution before and after adsorption on the bioactive glass without GA and with GA, with the resulting dipolar evolution function ($V(t)$, upper left inset), the form factor ($F(t)$, upper right inset) as well as the assumed Gaussian distance distribution $P(r)$.

DEER measurements showed that the polymerization of the protein occurs when it is attached to the BG treated with GA. It remains questionable whether the secondary structure of the protein changes in this situation. In this purpose, FTIR measurements were performed on the BG treated with GA, in order to obtain information about the changes in secondary structure of methemoglobin after adsorption. FTIR spectra recorded before and after protein adsorption are shown in figure 4. In order to monitor the protein adsorption over time, we compared FTIR spectra recorded for BG immersed in protein solution for different periods of time: 10 min, 20 min, 30 min and 2 hours respectively. The amide I intensity increases with time immersion, and consequently with the amount of the protein attached on the BG, proving that the intensity of amide I band can be taken as a measure of the quantity of adsorbed protein (figure 4).

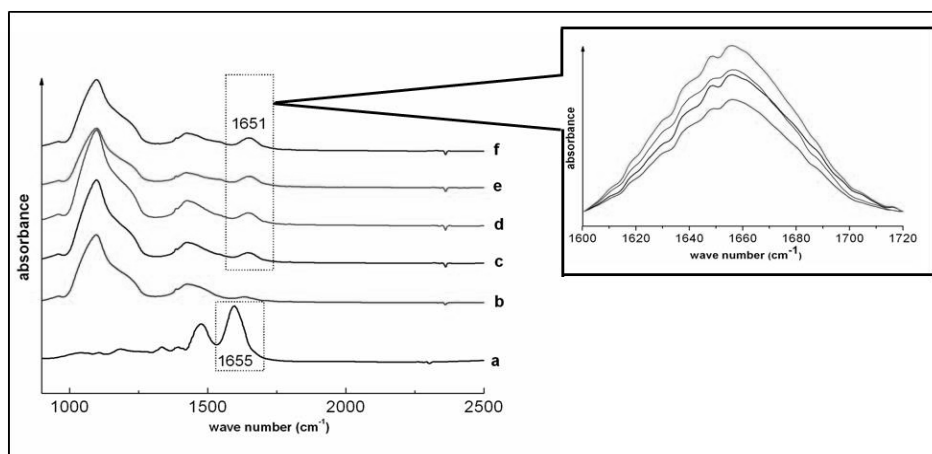


Figure 4. FTIR spectra (region 750-2000 cm^{-1}) of BG treated with GA (b), horse methemoglobin before (a) and after adsorption on BG with GA, after 10 min (c), 20 min (d), 30 min (e) and 2h (f) of immersion in protein solution. The amide I area is highlighted by the dashed line. The area enlarged in the upper right: separation of the amide I band of methemoglobin in adsorbed state, after the removal of corresponding band of the BG.

The FTIR signal characteristic to amide I functional group was located at 1655 cm^{-1} for lyophilized horse hemoglobin and 1651 cm^{-1} in case of the protein attached to the BG. The resulting component bands of amide I were assigned to different elements of the secondary structure, depending on their frequency. A Gaussian curve fitting procedure was applied to estimate quantitatively the area of each component representing a type of secondary structure. Peak locations were determined from the second derivative of the amide I band. In case of the protein in the adsorbed state, the BG signal was

prior subtracted, to eliminate the BG contribution in the amide I region. The results of the curve-fitting spectrum of amide I band are shown in figure 5 and the contribution of each element of the secondary structure is shown in figure 6. Hemoglobin is a α -helical protein and contains no β -structure [35]. The small peaks at ca. 1627 and 1638 cm^{-1} can therefore be assigned to β -turns (it can be associated with the short, extended chains connecting the helical cylinders) [36]. The pronounced peak between 1656-1658 cm^{-1} can be assigned to α -helices. The peak which appears around 1615 cm^{-1} is not related to the secondary structure and probably caused by other side-chain residues (it can be associated with tyrosine residues) [36]. The prediction of α -helix contribution determined from the amide I region is similar to other studies [37, 38]. The helix content of horse methemoglobin adsorbed on the BG treated with GA was found to be aprox. 4% lower than in the native protein, while the content of turns and random coil increased with 2% each.

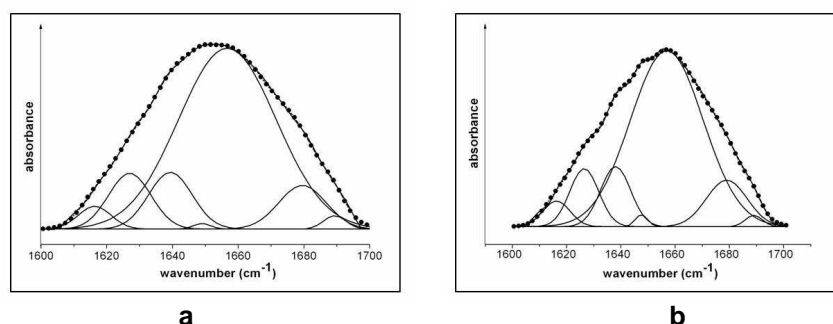


Figure 5. Separation of the amide I band into its components for the protein before **(a)** and after **(b)** adsorption on the BG treated with GA. The line with circle symbols represents the sum of the separated band components.

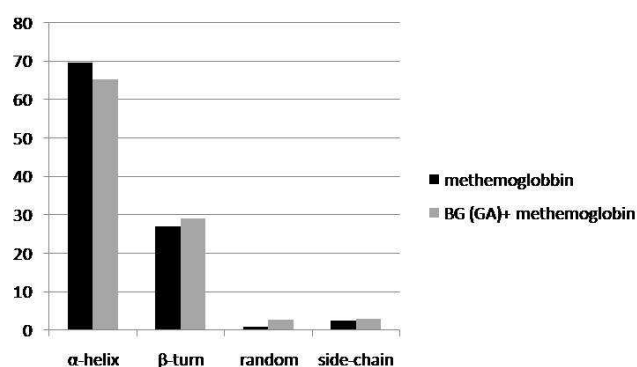


Figure 6. Relative percentage of secondary structure elements determined from amide I deconvolution for horse methemoglobin in native state (black) and after adsorption (gray) on BG with GA.

CONCLUSIONS

In this work EPR and FTIR measurements were carried out to study the adsorption of methemoglobin on bioactive glass system. Cw-EPR measurements confirmed that the protein immobilization is increasing in the adsorbed state while from DEER measurements we could conclude that a small fraction of protein dissociates after adsorption and GA induces polymerization of methemoglobin. FTIR experiments have shown that only small changes occur in the secondary structure of the protein in upon adsorption.

EXPERIMENTAL SECTION

Bioactive glass preparation

The bioactive glass was prepared via sol-gel method with the following composition (in weight %): 45% SiO₂, 24.5% Na₂O, 24.5% CaO and 6% P₂O₅. After preparation, the BG was milled and the obtained powder had particles with size between 500 nm and 1.5 µm. Further on, the BG powder was surface functionalized by following the protocol presented in other studies [7,8,24,25]. First, the powder was immersed for 4 hours into an aqueous APTS solution (0.45mol/L, pH adjusted to 8 by adding 1M HCl) at 80°C. After 4h the sample was collected, washed in deionised water, then immersed for 1h in GA solution (1mol/L) at room temperature and finally washed again in deionised water.

Spin labeling

Oxyhemoglobin was extracted from fresh horse blood samples according to Benesch et al. [26], and then converted to methemoglobin by addition of a 2-fold amount of K₃Fe(CN)₆ [27]. Spin labeling of the methemoglobin with (4-(2-Iodoacetamido)-2,2,6,6-tetramethyl-1-piperidinyloxy) (JAA6) followed the procedure of McCalley et al. [28].

Protein adsorption

Powder samples were incubated at 37°C for 10 min, 20 min, 30 min and 2 hours respectively, in a solution of 150 mg/ml (2.32 mM) methemoglobin in phosphate buffer (0.01M, pH 8.0) with 500mM NaCl concentration. This protein concentration was chosen because it is in the range of the concentration of hemoglobin in horse blood (between 150-200 mg/ml). After the immersion the samples were washed three times with the buffer solution. For the FTIR measurements the samples were lyophilized for 48 hours in an Alpha 1-2 LD type freeze dryer at 217K and 0.05mbar.

FTIR spectroscopy

FTIR spectroscopic analyses were performed in reflection configuration by a Jasco IRT-5000 FT-IR microscope in the range 4000-650 cm⁻¹ with a

resolution of 4 cm^{-1} . In order to subtract the background signal of the BG in the amide I region, the weight of the sample was the same for the spectra recorded on samples containing BG (0.73mg).

EPR SDSL spectroscopy

For the X-band continuous wave (cw) EPR measurements sample volumes of $15 \text{ }\mu\text{l}$ (BG + protein) were filled into EPR glass capillaries with 0.9 mm inner diameter (the active volume of the sample tube is $10 \text{ }\mu\text{l}$). The cw-EPR experiments were performed using a home-made EPR spectrometer equipped with a Bruker dielectric resonator. The microwave power was set to 1.0 mW , the B-field modulation amplitude was 0.15 mT .

Pulse EPR measurements were accomplished at 50 K , in X-band frequencies ($9.3\text{-}9.4 \text{ GHz}$) with a Bruker Eleksys 580 spectrometer equipped with a Bruker Flexline split-ring resonator ER 4118XMS3 and a continuous flow helium cryostat (ESR900, Oxford Instruments) controlled by an Oxford Intelligent temperature controller ITC 503S. Prior to freezing the protein in 3mm inner diameter EPR tubes, the samples had about 10% (by volume) glycerol. The measurements were performed using the four-pulse DEER sequence [29]:

$$\frac{\pi}{2}(\vartheta_{\text{obs}}) - \tau_1 - \pi(\vartheta_{\text{obs}}) - t' - \pi(\vartheta_{\text{pump}}) - (t_1 + t_2 - t') - \pi(\vartheta_{\text{obs}}) \\ - \tau_2 - \text{echo}$$

All measurements were performed at a temperature of 50 K with observer pulse lengths of 16 ns for $\frac{\pi}{2}$ and 32 ns for π pulses and a pump pulse length of 12 ns . Data points were collected in 8-ns time steps. The total measurement time for each sample was $4\text{--}24 \text{ h}$. Analysis of the data was performed with DeerAnalysis2009 [30].

ACKNOWLEDGMENTS

This research was accomplished in the framework of the PNII Idei PCCE-312 /2008 project granted by the Romanian National University Research Council. C.G. acknowledges the financial support from a program co-financed by The SECTORAL OPERATIONAL PROGRAMME HUMAN RESOURCES DEVELOPMENT, Contract POSDRU 6/1.5/S/3 – „Doctoral studies: through science towards society”.

REFERENCES

1. C.C. Berry, S. Adams, G. Curtis, *Journal of Physics D Applied Physics*, **2003**, 36, 198.
2. C.T. Shibata, A.M. Lenhoff, *Journal of Colloid and Interface Science*, **1992**, 148, 469.
3. C.T. Shibata, A.M. Lenhoff, *Journal of Colloid and Interface Science*, **1992**, 148, 485.
4. J. Hermans, H. Scheraga, *Journal of the American Chemical Society*, **1961**, 83, 3283.
5. M. Heule, K. Rezwan, L. Cavalli, L.J. Gauckler, *Advanced Materials*, **2003**, 15, 1191.
6. H.H. Weetall, "Covalent Coupling Methods for Inorganic Support Materials Methods in Enzymology", Methods in Enzymology Vol. 44, *Academic Press*, New York, **1976**.
7. Q.Z. Chen, K. Rezwan, V. Françon, D. Armitage, S.N. Nazhat, F.H. Jones, A.R. Boccaccini, *Acta Biomaterialia*, **2007**, 3, 551.
8. R.A. Williams, H.W. Blanch, *Biosensors and Bioelectronics*, **1994**, 9, 159.
9. R.W. Sarver Jr., W.C. Krueger, *Analytical Biochemistry*, **1991**, 194, 89.
10. A. Dong, P. Huang, W.S. Caughey, *Biochemistry*, **1990**, 29, 3303.
11. A. Dong, W.S. Caughey, T.W. Du Clos, *The Journal of Biological Chemistry*, **1994**, 269, 6424.
12. R.W. Sarver Jr., W.C. Krueger, *Analytical Biochemistry*, **1993**, 212, 519.
13. J. Buijs, W. Norde, J.W.Th. Lichtenbelt, *Langmuir*, **1996**, 12, 1603.
14. S.S. Cheng, K.K. Chittur, C.N. Sukenik, L.A. Culp, K. Lewandowska, *Journal of Colloid and Interface Science*, **1994**, 162, 135.
15. L.A. Buchanan, A. El-Ghannam, *Journal of Biomedical Materials Research Part A*, **2009**, 93A, 537.
16. C.E. Giacomelli, M.G.E.G. Bremer, W. Norde, *Journal of Colloid and Interface Science*, **1999**, 220, 13.
17. B. Stuart, "Biological Applications of Infrared Spectroscopy", John Wiley & Sons, Chichester, **1997**.
18. K. Jacobsen, S. Oga, W.L. Hubbell, T. Risse, *Biophysical Journal*, **2005**, 88, 4351.
19. T. Risse, W.L. Hubbell, J.M. Isas, H.T. Haigler, *Physical Review Letters*, **2003**, 91, 188101.
20. K. Jacobsen, W.L. Hubbell, O.P. Ernst, T. Risse, *Angewandte Chemie International Edition*, **2006**, 45, 3874.
21. E. Bordignon, H.J. Steinhoff, "Membrane protein structure and dynamics studied by side-directed spin labeling ESR", *ESR Spectroscopy in Membrane Biophysics*, Springer Science and Business Media, New York, **2007**.
22. J.P. Klare, H.J. Steinhoff, *Photosynthesis Research*, **2009**, 102, 377.
23. J.P. Klare, H.J. Steinhoff, "Site-directed Spin Labeling and Pulsed Dipolar Electron Paramagnetic Resonance", *Encyclopedia of Analytical Chemistry*, Chichester, **2010**.

24. Q.Z. Chen, K. Rezwan, D. Armitage, S.N. Nazhat, A.R. Boccaccini, *Journal of Materials Science: Materials in Medicine*, **2006**, 17, 979.
25. A. Nanci, J.D. Wuest, L. Peru, P. Brunet, V. Sharma, S. Zalzal, M.D. McKee, *Journal of Biomedical Materials Research*, **1998**, 40, 324.
26. R.E. Benesch, R. Benesch, R.D. Renthal, N. Maeda, *Biochemistry*, **1972**, 11, 3576.
27. H.J. Steinhoff, K. Lieutenant, A. Redhardt, *Biochimica et Biophysica Acta*, **1989**, 996, 49.
28. R.C. McCalley, E.J. Shimshick, H.M. McConnell, *Chemical Physics Letters*, **1972**, 13, 115.
29. M. Pannier, S. Veit, A. Godt, G. Jeschke, H.W. Spiess, *Journal of Magnetic Resonance*, **2000**, 142, 331.
30. G. Jeschke, V. Chechik, P. Ionita, A. Godt, H. Zimmermann, J. Banham, C.R. Timmel, D. Hilger, H. Jung, *Applied Magnetic Resonance*, **2006**, 30, 473.
31. Moffat JK, *Journal of Molecular Biology*, **1971**, 55, 135.
32. C. Gruian, H.J. Steinhoff, S. Simon, *Digest Journal of Nanomaterials and Biostructures*, **2011**, 6, 373.
33. D.E. Budil, S. Lee, S. Saxena, J.H. Freed, *Journal of Magnetic Resonance Series A*, **1996**, 120, 155.
34. J. McGuire, V. Krisdhasima, M.V. Wahlgren, T. Arnebrant, "Proteins at interfaces II, Vol. 602", American Chemical Society, Washington, **1995**.
35. **M. Levitt, J. Greer**, *Journal of Molecular Biology*, **1977**, 114, 181.
36. H. Susi, D.M. Byler, *Biochemical and Biophysical Research Communications*, **1983**, 115, 391.
37. S. Cai, B.R. Singh, *Biochemistry*, **2004**, 43, 2541.
38. S. Luo, C-Y.F. Huang, J.F. McClelland, D.J. Graves, *Analytical Biochemistry*, **1994**, 216, 67.